Soft Matter

PAPER

Supporting Information

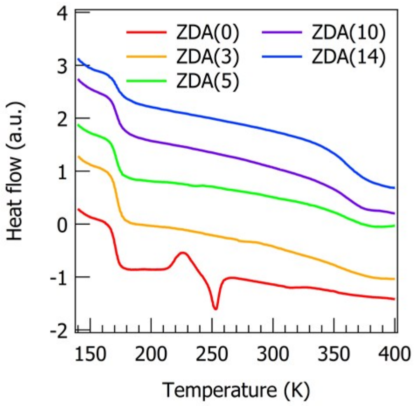

Figure SI DSC curves of ZDA(0) (–), ZDA(3) (–), ZDA(5) (–), ZDA(10) (–), and ZDA(14) (–). The crystallization and melting peaks were seen only in the DSC curve of ZDA(0), and there is no peak from 210 to 250 K for other samples. The peaks observed at 210 - 250 K for ZDA(0) were originated from crystallization and melting peaks due to high *cis* content in present BR. No peculiar behavior is seen in ZDA(0) compared with other samples in elastic scattering measurements, suggesting that there is little or none effect of crystallization on the results from ZDA(0) in present QENS experiment.

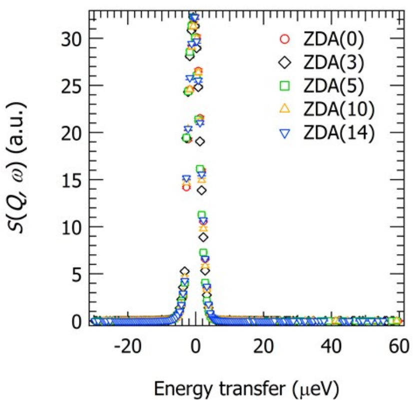

Figure SII Dynamic scattering laws $S(Q, \omega)$ for ZDA(0) (○), ZDA(3) (◇), ZDA(5) (□), ZDA(10) (△) and ZDA(14) (▽) at 10 K, defined as the resolution function, in the range Q = 1.48 Å^{-1}. FWHM obtained by fitting, corresponding to the energy resolution δE in the present study, is 4.0 ± 0.2 μeV. The resolution functions are almost the same between samples.

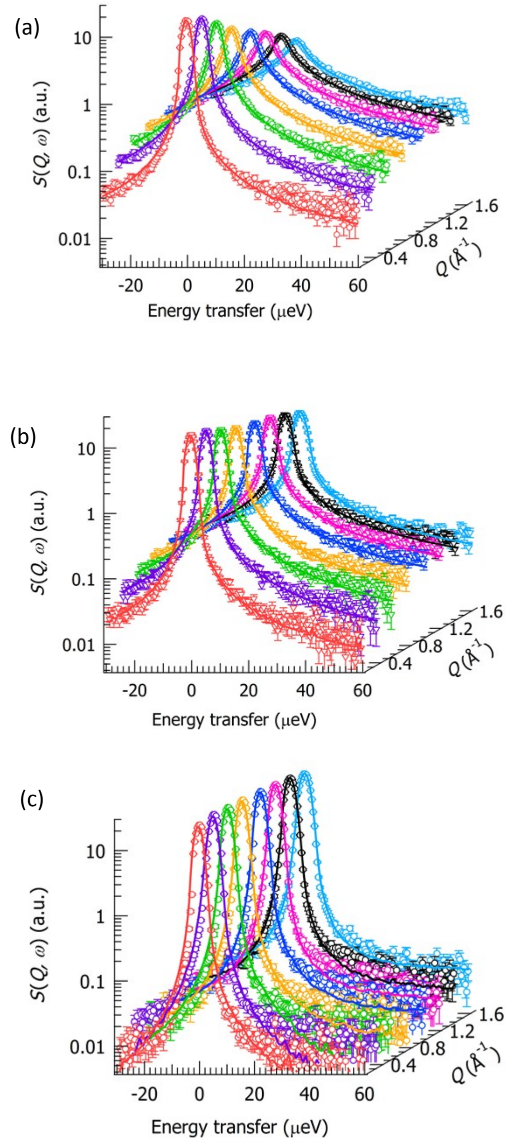

Figure SIII Fitting results of $S(Q, \omega)$ for (a) ZDA(0) at 310 K, (b) ZDA(14) at 310K and (c) ZDA(0) at 200 K in the range Q = 0.23 (○ and ▽), Q = 0.43 (○ and ▽), Q = 0.63 (○ and ▽), Q = 0.83 (○ and ▽), Q = 1.08 (○ and ▽), Q = 1.28 (○ and ▽), Q = 1.48 (○ and ▽) and Q = 1.68 (○ and ▽). Solid lines are the results of fitting with calculations by Eq. (2). $S(Q, \omega)$ are fitted fairly well by Eq. (2) in various Q ranges.

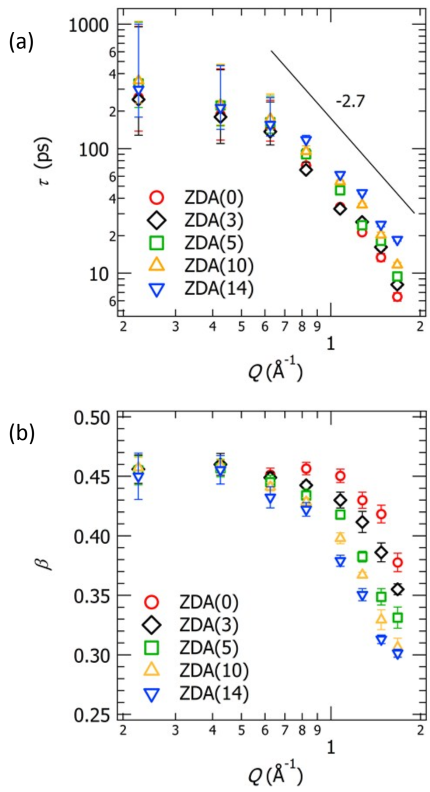

Figure SIV Q dependence of (a) the relaxation time τ and (b) relaxation time distribution β obtained by fittings with Eq. (2) for ZDA(0) (○), ZDA(3) (◇), ZDA(5) (□), ZDA(10) (△) and ZDA(14) (▽) at 310 K. The increase of τ and the decrease of β with an increase in the ZDA volume fraction were observed in the range $Q > 0.65$ Å^{-1}.

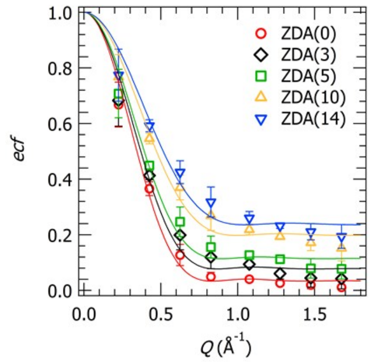

Figure SV Q dependence of *ecf* for ZDA(0) (○), ZDA(3) (◇), ZDA(5) (□), ZDA(10) (△) and ZDA(14) (▽) at 310 K. Solid lines are the fitting results with the diffusion inside a sphere model[32-34], which works only for monodisperse systems (Eq. (SI I)).

$$ecf = P + (1-P)\left[\frac{3j_1(Qr)}{(Qr)}\right]^2, \qquad \text{(SI I)}$$

where P, $j_1(Qr)$ and r are the fraction of immobile component which are dynamically inactive at a given temperature, the spherical Bessel function of the first order, and the radius of the confining sphere, respectively. Although ZDA/BR system is not dynamically homogenous but rather heterogeneous one, we try to adopt a model assuming that present system is dynamically homogeneous because of the inability to decouple *ecf* from mobile, immobile, and intermediate phase. Fitting parameters are listed in Table SI. P increases and r decreases with increasing the ZDA volume fraction. Namely, the increase in the immobile component and the decrease of hopping distance of mobile component were found with increases in the ZDA volume fraction.

Table SI Summary of fitting parameters of Q dependence of *ecf* at 310 K.

	ZDA(0)	ZDA(3)	ZDA(5)	ZDA(10)	ZDA(14)
P	0.03±0.018	0.08±0.023	0.11±0.022	0.20±0.023	0.24±0.026
r (Å)	5.39±0.024	5.20±0.031	5.04±0.030	4.52±0.029	4.31±0.030

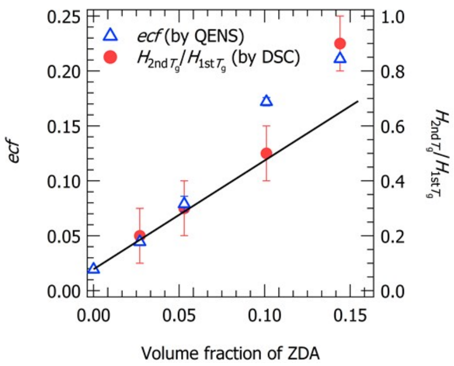

Figure SVI *ecf* (△) and $H_{2nd\ Tg}/H_{1st\ Tg}$ (●) as a function of volume fraction of ZDA. $H_{2nd\ Tg}/H_{1st\ Tg}$ is the ratio between the step heights of first T_g ($H_{1st\ Tg}$) and second T_g ($H_{2nd\ Tg}$) obtained from DSC curves. As $H_{2nd\ Tg}/H_{1st\ Tg}$ increases with increasing the volume fraction of ZDA, second T_g must be originated from HC-BR segregated around ZDA aggregates. *ecf* exhibits similar dependency of $H_{2nd\ Tg}/H_{1st\ Tg}$ qualitatively. In addition, it can be clearly seen that elastic modulus drastically increased above the volume fraction of ZDA of 0.05 as shown in Figure 2. Hence, the consistency between elastic modulus, $H_{2nd\ Tg}/H_{1st\ Tg}$, and *ecf* leads the plausible structural-dynamical-mechanical picture of ZDA/BR.